Biochimica et Biophysica Acta 1832 (2013) 660–673

Contents lists available at SciVerse ScienceDirect

Biochimica et Biophysica Acta

journal homepage: www.elsevier.com/locate/bbadis

Protective effects of lipocalin-2 (*LCN2*) in acute liver injury suggest a novel function in liver homeostasis☆,☆☆

Erawan Borkham-Kamphorst [a,*], Eddy van de Leur [a], Henning W. Zimmermann [b], Karlin Raja Karlmark [b], Lidia Tihaa [a], Ute Haas [a], Frank Tacke [b], Thorsten Berger [c], Tak W. Mak [c], Ralf Weiskirchen [a,*]

[a] Institute of Clinical Chemistry and Pathobiochemistry, RWTH Aachen University Hospital, Germany
[b] Department of Medicine III, RWTH Aachen University Hospital, Germany
[c] The Campbell Family Institute for Breast Cancer Research and the Ontario Cancer, Institute, University Health Network, Toronto, ON, Canada

ARTICLE INFO

Article history:
Received 16 November 2012
Received in revised form 10 January 2013
Accepted 16 January 2013
Available online 31 January 2013

Keywords:
Lipocalin
LCN2
NGAL
BDL
CCl_4
Acute phase response

ABSTRACT

Lipocalin-2 is expressed under pernicious conditions such as intoxication, infection, inflammation and other forms of cellular stress. Experimental liver injury induces rapid and sustained LCN2 production by injured hepatocytes. However, the precise biological function of LCN2 in liver is still unknown. In this study, $LCN2^{-/-}$ mice were exposed to short term application of CCl_4, lipopolysaccharide and Concanavalin A, or subjected to bile duct ligation. Subsequent injuries were assessed by liver function analysis, qRT-PCR for chemokine and cytokine expression, liver tissue Western blot, histology and TUNEL assay. Serum LCN2 levels from patients suffering from liver disease were assessed and evaluated. Acute CCl_4 intoxication showed increased liver damage in $LCN2^{-/-}$ mice indicated by higher levels of aminotransferases, and increased expression of inflammatory cytokines and chemokines such as IL-1β, IL-6, TNF-α and MCP-1/CCL2, resulting in sustained activation of STAT1, STAT3 and JNK pathways. Hepatocytes of $LCN2^{-/-}$ mice showed lipid droplet accumulation and increased apoptosis. Hepatocyte apoptosis was confirmed in the Concanavalin A and lipopolysaccharide models. In chronic models (4 weeks bile duct ligation or 8 weeks CCl_4 application), $LCN2^{-/-}$ mice showed slightly increased fibrosis compared to controls. Interestingly, serum LCN2 levels in diseased human livers were significantly higher compared to controls, but no differences were observed between cirrhotic and non-cirrhotic patients. Upregulation of LCN2 is a reliable indicator of liver damage and has significant hepato-protective effect in acute liver injury. LCN2 levels provide no correlation to the degree of liver fibrosis but show significant positive correlation to inflammation instead.

1. Introduction

Lipocalins are a distinct family of over thirty small soluble secreted proteins involved in the transport of small hydrophobic proteins [1]. Although most of these proteins share three conserved motifs, they have a large degree of diversity with limited regions of sequence homology. However, they contain a single characteristic eight-stranded, continuously hydrogen-bonded anti-parallel β-barrel [1]. Lipocalin-2 (LCN2) also known as 24p3 protein was first identified in urine taken from mice with SV40-infected kidneys [2]. Neutrophil gelatinase-associated lipocalin (NGAL), the human homologue of LCN2, was subsequently purified from neutrophils and shown to be associated with gelatinase that does not directly affect its enzymatic activity [3]. Rodent forms of this lipocalin are not associated with gelatinase, and most NGAL is exocytosed from neutrophils in a form that is not complexed with gelatinase [3]. Several functions of LCN2 have been identified, but the precise cellular and extracellular roles are not yet defined. Functions related to cancer have been suggested [4–6], but overall, the role of LCN2 in cell signaling, proliferation, and apoptosis is still unclear. Some data suggest a role in inflammation [7], while other studies point at an important LCN2 role in iron metabolism [8]. A number of inducers of this gene have been found, including serum, lipopolysaccharide (LPS), various growth factors, retinoic acid, glucocorticoids, and phorbol esters [4,9]. Also MK-886, nordihydroguaiaretic acid (NDGA), and several compounds acting as cyclooxygenase-2 inhibitors that induce apoptosis stimulate LCN2 expression [10,11]. LCN2 may serve as an acute kidney injury biomarker [12] and exhibits important beneficial functions in renal damage in experimental ischemia–reperfusion injury [13,14]. It induces iron-dependent responses, possibly *via* renal epithelial

Abbreviations: HRS, hepatorenal syndrome; NGAL/LCN2, lipocalin 2 protein; LPS, lipopolysaccharide; ConA, Concanavalin A; BDL, bile duct ligation; MCP-1/CCL2, monocyte chemoattractant protein-1/C–C chemokine ligand-2

☆ Conflict of interest: None of the authors have something to declare.

☆☆ Financial support: This work was supported by grants from the Deutsche Forschungsgemeinschaft (SFB/TRR57, P13) and the IZKF Aachen of the RWTH Aachen University.

* Corresponding authors at: Institute of Clinical Chemistry and Pathobiochemistry, RWTH-University Hospital, D-52074 Aachen, Germany. Tel.: +49 241 8088683; fax: +49 241 8082512.

E-mail addresses: ekamphorst@ukaachen.de (E. Borkham-Kamphorst), rweiskirchen@ukaachen.de (R. Weiskirchen).

0925-4439/$ – see front matter © 2013 Elsevier B.V. All rights reserved.
http://dx.doi.org/10.1016/j.bbadis.2013.01.014

delivery of catechol–iron complexes [15]. Hence, LCN2 may comprise an endogenous nephron-protective mechanism limiting repeated bouts of tubular insult [16]. In contrast, LCN2 is on the other hand reported to be essential for chronic kidney disease progression in mice and humans [17].

In murine liver, LCN2 is markedly induced during experimental sepsis and supposed to participate in antimicrobial host defenses by binding and scavenging bacterial iron-containing siderophores [18–21]. We recently identified that LCN2 is induced during experimental liver injury [22]. Moreover, immunohistochemistry and cell-based experiments revealed that injured hepatocytes are the main source of hepatic LCN2 [22]. Previous findings further suggest that LCN2 is induced in heart, kidney and liver after X-ray exposure most likely by the activity of reactive oxygen species [23].

To further elucidate the causes of LCN2 induction and its functioning, we here performed a set of experiments in different models of experimental liver injury. LCN2$^{-/-}$ mice were subjected to acute and chronic liver injury by application of CCl_4, Concanavalin A (ConA), LPS and ligation of the common bile duct (BDL). Acute single dose CCl_4 intoxication showed more liver damage in LCN2$^{-/-}$ mice indicated by significant higher levels of aminotransferases and increased expression of inflammatory cytokines and chemokines including IL-1β, TNF-α and the monocyte chemoattractant protein-1/C–C chemokine ligand-2 (MCP-1/CCL2). Additionally, hepatocytes of LCN2$^{-/-}$ mice showed enhanced hepatic lipid droplet accumulation and apoptosis. Increased apoptosis in LCN2 deficient mice was also found after application of ConA or LPS and in livers of animals that were subjected to BDL for five days. During chronic insult, LCN2$^{-/-}$ mice showed more severe fibrosis compared to wild type controls. In humans, patients with chronic liver disease displayed overall higher serum LCN2 levels that were associated with impaired renal function.

2. Material and methods

2.1. Primary liver cell isolation and culturing

Hepatocytes were isolated using the collagenase method of Seglen as described previously [24] and cultured on collagen-coated dishes in Hepatozyme-SFM medium (Gibco, Invitrogen, St. Louis, MO).

2.2. RNA isolation, RT-PCR, and qRT-PCR

Total RNA from hepatocytes and liver tissue were isolated through QIAzol Lysis Reagent containing a monophasic solution of phenol and guanidine thiocyanate, followed by chloroform and isopropanol precipitation, DNAse digestion and RNeasy clean up with Mini Kits (Qiagen, Hilden, Germany). Amplification primers were selected from sequences deposited in the GenBank database (Table 1) using the Primer Express software (Applied Biosystems Invitrogen, Darmstadt, Germany).

Table 1
Primers used in this study.

Gene[1]	Acc. no.	Forward primer	Reverse primer
Col αI	NM_007742	catgttcagctttgtggacct	gcagctgacttcagggatgt
α-SMA	NM_009606	aatgagcgtttccgttgc	atccccgcagactccatac
IL-1α	NM_010554	ttggttaaatgacctgcaaca	gagcgctcacgaacagttg
IL-1β	NM_008361	gagctgaaagctctccacctc	ctttcctttgaggcccaaggc
IL-6	NM_031168	gctaccaaactggatataatcagga	ccaggtagctatggtactccagaa
TNF-α	NM_013693	accacgctcttctgtctactga	tccacttggtggtttgctacg
CCL2	NM_011333	gtgttggctcagccagatgc	gacacctgctgctggtgatcc
CCR2	NM_009915	tcgctgtaggaatgagaagaagagg	caaggattcctggaaggtggtcaa
IFN-γ	NM_008337	ggaggaactggcaaaaggatgg	tgttgctgatggcctgattgtc
IL-2	NM_008366	gctgttgatggacctacagga	ttcaattctgtggcctgctt
IL-4	NM_021283	cgtcctcacagcaacgaagaagcac	aagagtctctgcagctccatga
IL-10	NM_010548	ggctgaggcgctgtcatcg	tcattcatggccttgtagacacc
β-Actin	NM_007393	ctctagacttcgagcaggagatgg	atgccacaggattccatacccaaga
rS6	BC092050	cccatgaagcaaggtgttct	acaatgcatccacgaacaga

First-strand cDNA was synthesized from 1 μg RNA in 20 μl volume using SuperScriptTM II RNAse H reverse transcriptase and random hexamer primers (Invitrogen). First-strand cDNA derived from 25 ng RNA was subjected to real-time quantitative PCR, using qPCR Core Kits (Eurogentec, Cologne, Germany). PCR conditions were 50 °C for 2 min, 95 °C for 10 min and 40 cycles of 95 °C for 15 s and 60 °C for 1 min. All Taqman primers used in this study are given in Table 1. RNA normalization was obtained through Taqman Ribosomal RNA Control Reagents (Applied Biosystems) designed for 18S ribosomal RNA (rRNA) detection.

2.3. Patient samples

We included patients with chronic liver diseases of any etiology, who were treated at our hospital as in- or outpatients [25]. Informed consent was obtained prior to recruitment. A total of n = 192 serum specimens was analyzed encompassing patients without fibrosis, patients with histologically proven fibrosis and individuals that were diagnosed for cirrhosis based on the conjunction of imaging studies, liver histology, laboratory parameters and the presence of typical cirrhosis-related sequela [25]. Cirrhotic patients were further stratified according to the Child–Turcotte–Pugh-Score [26]. Healthy blood donors (n = 91) from the local blood bank served as controls.

2.4. Animal experiments and specimen collection

All animal protocols were in full compliance with the guidelines for animal care approved by the German Animal Care Committee.

a) acute injury models: To investigate the effect of LCN2 in acute liver injury in mice, we used 6–8 week-old C57BL/6 wild type and LCN2$^{-/-}$ mice subjected to either (i) a single intraperitoneal injection of 0.8 ml/kg body weight CCl_4 (in mineral oil) for 48 h or (ii) a single intravenous injection of 20 mg/kg body weight ConA (Sigma, Taufkirchen, Germany) for 8 or 24 h or the respective tracer controls, as previously described [27], (iii) single dose i.p. of LPS (2.5 mg/kg) for 2 and 6 h respectively and (iv) 5 day-BDL [28,29].
b) chronic injury models: For chronic liver injury, we used long term application of CCl_4 for 8 weeks or BDL for 4 weeks. Mice were sacrificed, serum samples analyzed by standard techniques and liver specimens snap frozen in liquid nitrogen for protein and RNA isolation. Frozen tissue section were preserved with Tissue-Tek (Sakura Finetek, The Netherlands) in ice-cold 2-methylbutane (Roth, Karlsruhe, Germany) and kept at −80 °C, or fixed in 4% buffered paraformaldehyde for histological examination.

2.5. Immunohistochemistry

Paraffin-embedded liver tissue sections were treated as described [30]. Non-specific staining was blocked with 50% FCS and 0.3% Triton X-100 in PBS for 30 min at 37 °C followed by incubation with peroxidase, avidin and biotin. Blots were incubated with primary antibodies at 4 °C overnight followed by incubation with biotinylated secondary antibodies (BA-9200, Vector Laboratories, Eching, Germany), avidin-conjugated peroxidase (Vectastain ABC-Elite reagent, Vector Laboratories) and developed using the 3,3′-diaminobenzidine substrate (DAKO, Hamburg, Germany).

2.6. SDS-PAGE and Western blot analysis

Cell and tissue lysates were prepared using RIPA buffer containing 20 mM Tris–HCl (pH 7.2), 150 mM NaCl, 2% (w/v) NP-40, 0.1% (w/v) SDS, 0.5% (w/v) sodium deoxycholate and the Complete™-mixture of proteinase inhibitors (Roche Diagnostics, Mannheim, Germany). Equal amounts of cellular or liver protein extracts were diluted with Nu-PAGE ™ LDS electrophoresis sample buffer and DTT as reducing agent, then heated at 95 °C for 10 min. and separated in 4–12% Bis–Tris gradient

Table 2
Antibodies used in this study.

Antibody	Cat no.	Supplier	Species[1]	Dilution
LCN2	AF3508	R&D Systems, Wiesbaden, Germany	m, r	1:1000
Phospho JNK	9251	Cell Signaling, NEB, Frankfurt, Germany	h, m, r	1:1000
Total JNK	9252	Cell Signaling	h, m, r	1:1000
Phospho p65	3033	Cell Signaling	h, m, r	1:1000
Total p65	sc-8008	Santa Cruz Biotech, Santa Cruz, CA, USA	h, m, r	1:1000
Phospho STAT1	5806	Cell Signaling	h, m, r	1:1000
Total STAT1	Sc-346	Santa Cruz	h, m, r	1:1000
Phospho STAT3	9134	Cell Signaling	h, m, r	1:1000
Total STAT3	4904	Cell Signaling	h, m, r	1:1000
Phospho-IKKα/β	2697	Cell Signaling	h, m. r	1:1000
IKKα	2682	Cell Signaling	h, m. r	1:1000
IκBα	sc-371	Santa Cruz	h, m. r	1:1000
Cleaved caspase-3	9664	Cell Signaling	h, m, r	1:1000
Collagen type I	PS065	Monosan, Uden, The Netherlands	m, r	1:1000
Fibronectin	AB1954	Millipore, Merck, Billerica, MA, USA	m, r	1:1000
β-Actin	A5441	Sigma, Taufkirchen, Germany	h, m, r	1:10,000
α-SMA	CBL1	Cymbus Biotech, Hampshire, UK	h, m, r	1:2000
Ribosomal rS6	2317	Cell Signaling	h, m, r	1:1000
GAPDH	sc-32233	Santa Cruz	h, m, r	1:1000

gels using MOPS or MES running buffer (Invitrogen). Proteins were electroblotted onto nitrocellulose membranes and equal loading and protein transfer verified by Ponceau S stain. Non-specific binding sites were blocked in TBS containing 5% (w/v) non-fat milk powder. All antibodies (see Table 2) were diluted in 2.5% (w/v) non-fat milk powder in Tris-buffered saline. Primary antibodies were visualized using horseradish peroxidase conjugated anti-mouse-, anti-rabbit- or anti-goat IgG (Santa Cruz Biotech, Santa Cruz, CA) and the SuperSignal chemiluminescent substrate (Pierce, Bonn, Germany).

2.7. Terminal transferase dUTP nick end-labeling assay (TUNEL)

For DNA fragmentation detection resulting from apoptotic signaling cascades, we used In Situ Cell Death Detection Kit Fluorescein (Roche) according to the manufacturer's instructions. The presence of nicks in the DNA was identified by terminal deoxynucleotidyl transferase (TdT), an enzyme that catalyzes the addition of labeling dUTPs. Frozen liver tissue sections were analyzed with fluorescence microscope for direct fluorescein.

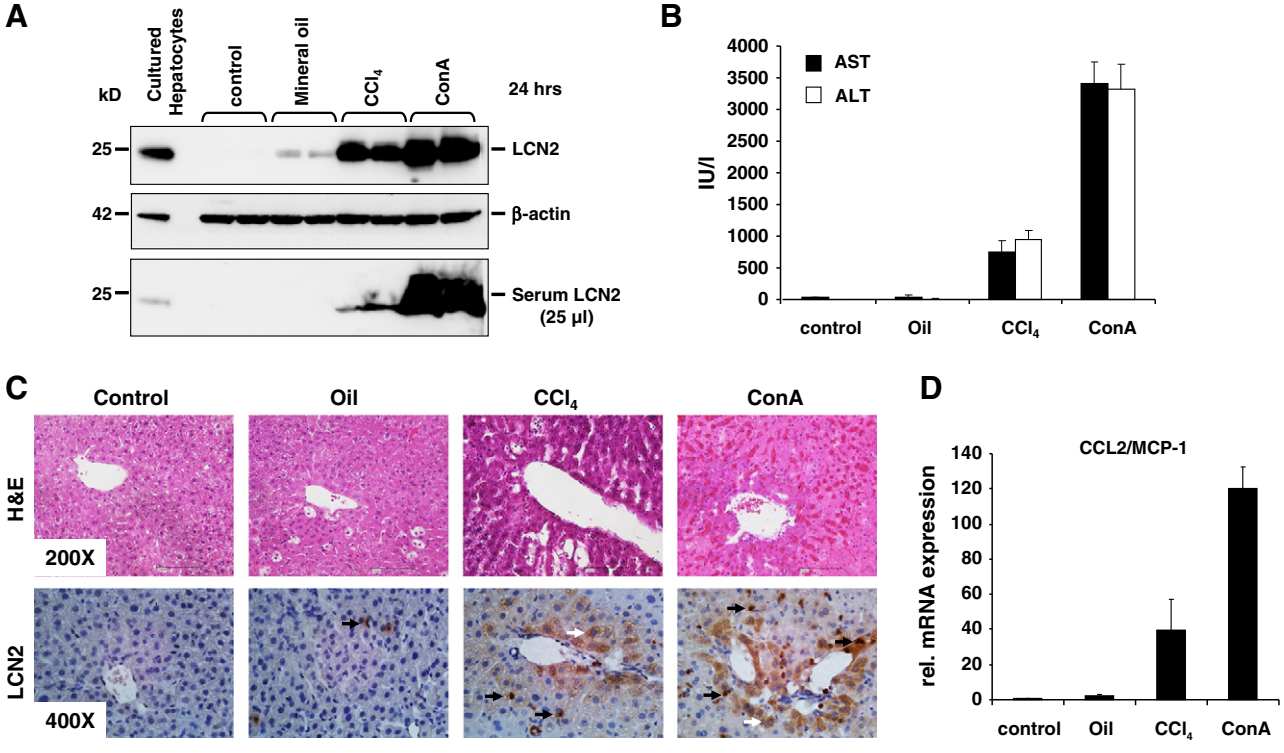

Fig. 1. LCN2 expression correlates with the degree of acute liver damage. (A) Liver lysates and serum samples of mice from different experimental models of liver injury were analyzed for LCN2 expression by Western blot, reflecting markedly increase of LCN2 24 h after CCl_4 and ConA injection. No LCN2 expression was found in untreated or mineral oil injected animals. (B) Elevated values of serum AST and ALT taken from animals 24 h after injection of CCl_4 and ConA indicate liver insult. Serum samples taken from animals that received no injection of hepatotoxins or adequate volumes of oil were taken as control. (C) Immunohistochemistry of liver slices of respective animals showed high LCN2 expression in hepatocytes (white arrows) and infiltrating inflammatory cells (black arrows), especially in the immune-mediated ConA model. (D) Relative mRNA expression of the monocyte chemoattractant protein-1/C–C chemokine ligand-2 (MCP-1/CCL2) levels showed a direct correlation with LCN2 culmination after CCl_4 or ConA injection.

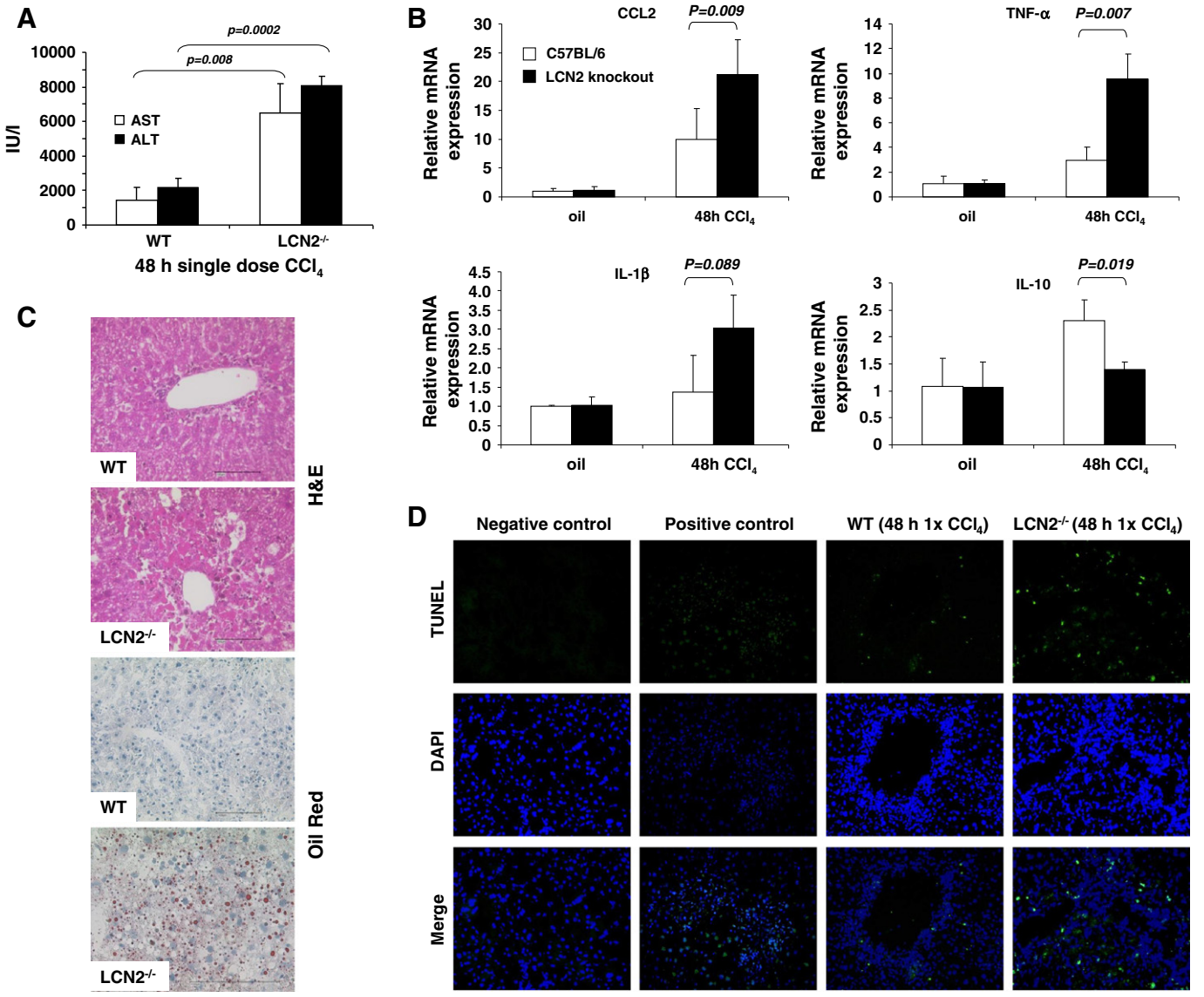

Fig. 2. LCN2 deficient mice show more liver damage after CCl_4 administration. (A) Wild type (C57BL/6) and LCN2$^{-/-}$ mice (6 animals/group) were treated with a single dose of CCl_4 (0.8 ml/kg) in mineral oil. Mice were sacrificed after 48 h and serum levels of AST and ALT determined. (B) Quantitative RT-PCR showed higher mRNA levels of inflammatory cytokines (i.e. CCL2, IL-1β, TNF-α, and IFN-γ) in LCN2$^{-/-}$ mice compared to controls, while the expression of IL-10 was reduced. (C) Hematoxylin/eosin and oil red staining showed increased liver damage and fat droplet accumulation in hepatocytes in LCN2 deficient mice compared to wild type controls. All black bars represent 100 μM. (D) TUNEL assay of acute CCl_4 liver injury showing increased hepatocyte apoptosis in LCN2$^{-/-}$ mice compared to controls.

2.8. Serum LCN2 ELISA measurements

Serum was 1:30 diluted and analyzed using the human lipocalin-2/NGAL ELISA kit (BioVendor, Brno, Czech Republic) according to the manufacturer's instructions.

2.9. Measurement of serum parameters

Serum biochemical parameters (ALT and AST) were measured using the Modular Pre-Analytics (MPA) system (Roche).

3. Results

3.1. LCN2 levels correlate with the degree of acute liver damage and inflammation

Our previous work suggested that upregulation of LCN2 after acute or chronic liver damage represents a distinct response of injured hepatocytes [22]. In mice, LCN2 is an acute-phase protein that appears rapidly in the bloodstream in response to a systemic infection or toxin exposure. Accordingly, LCN2 expression in mice is upregulated after injection of CCl_4- or ConA and correlates with hepatic injury indicated by elevated levels of AST and ALT (Fig. 1A, B). In contrast to normal tissue structure observed in control livers (injected with saline solution or mineral oil), a perivascular zone of necrosis was seen in livers of CCl_4-treated animals, while ConA-treated mice showed a diffuse perivascular and parenchymal zone of hepatic injury (Fig. 1C). Immunohistochemistry confirmed that LCN2 expression is induced in injured hepatocytes and infiltrating inflammatory cells (Fig. 1C). Interestingly, LCN2 induction was further associated with elevated expression of the inflammatory chemokine MCP-1/CCL2 (Fig. 1D).

The observed immunolocalization of LCN2 was in agreement with that observed in different other liver injury models in both rats and mice [22]. In the present mouse model, in which the expression of LCN2 was analyzed 6 h after LPS application, infiltrating inflammatory cells were the prominent cell type producing LCN2, while injured hepatocytes and inflammatory cells were found in both acute and chronic CCl_4 chemical injuries. Interestingly, our long-term mineral

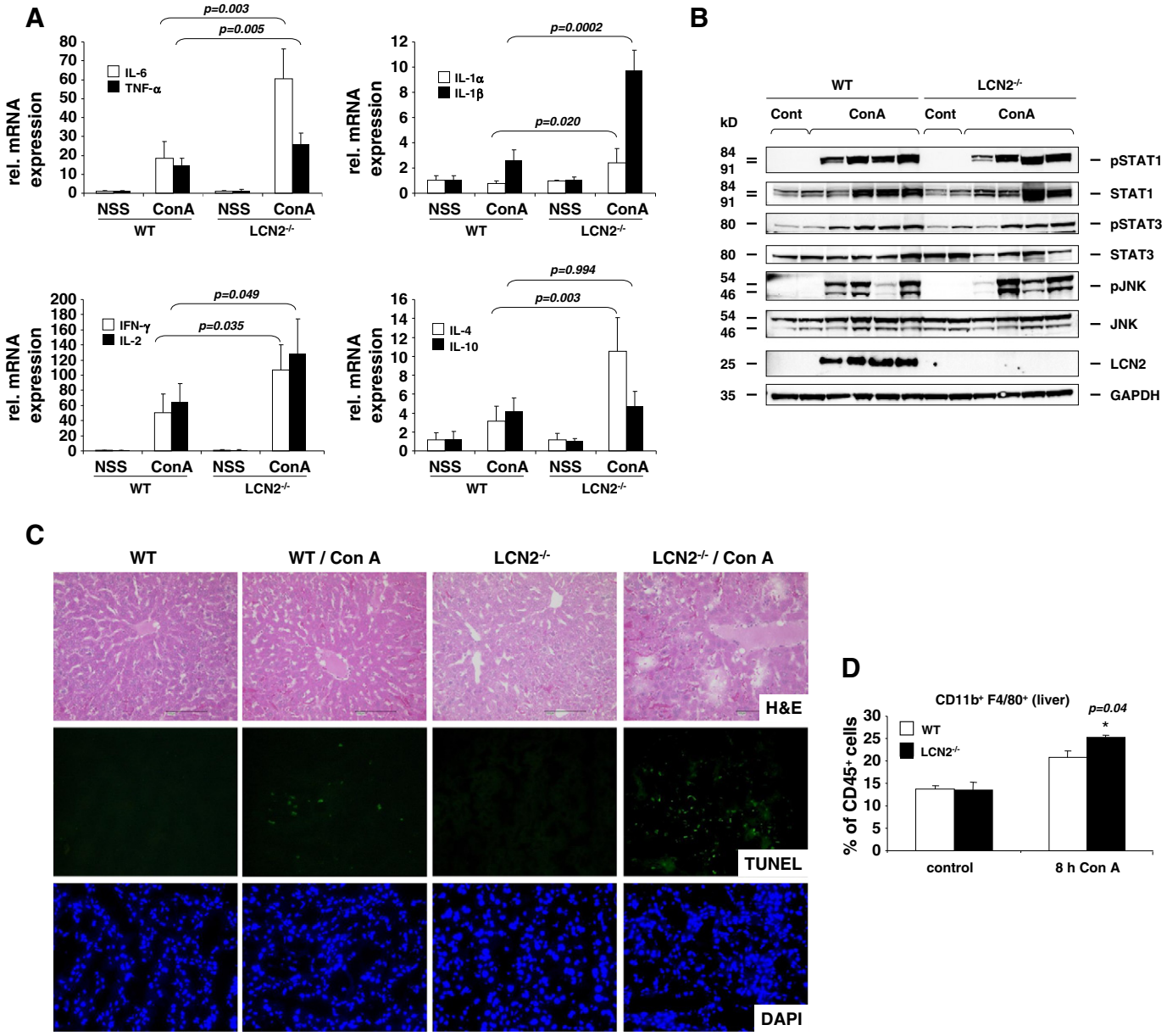

Fig. 3. LCN2$^{-/-}$ mice exhibit more injury in T-cell mediated ConA model of experimental liver injury. (A) qRT-PCR of liver RNA reflecting increased expression of the pro-inflammatory cytokines IL-6 and TNF-α (*upper left panel*), IL-1α and IL-1β (*upper right panel*) in LCN2$^{-/-}$ mice compared to the wild type controls. In addition, the Th1/Th2 cytokines IFN-γ and IL-2 (*lower left panel*) and IL-4 (*lower right panel*) also increased, while IL-10 (*lower right panel*) acting as an anti-inflammatory cytokine remained unchanged. (B) Western blot analysis confirmed the activation of respective signaling pathway during liver insult as shown by phosphorylation/activation of STAT1, STAT3 and JNK. (C) H&E staining and TUNEL assay of liver tissue showed that ConA increases liver damage and hepatocyte apoptosis in LCN2$^{-/-}$ animals. Black bars represent 100 μM. (D) FACS analysis of liver leukocyte isolates after ConA challenge showed higher levels of macrophages (CD11b^{+} F4/80^{+}) in LCN2-deficient mice.

oil i.p. injection control group showed diffused Kupffer cells and hepatic macrophages as the main source of LCN2 production. Furthermore, the BDL models showed a lesser degree of inflammation compared to the LPS- and CCl_4 models. Proliferative bile duct epithelia, hepatocytes and infiltrating inflammatory cells stained positive for LCN2 (Suppl. Fig. 1).

3.2. LCN2$^{-/-}$ mice are more susceptible to acute CCl_4-induced liver injury

Eight week-old C57BL/6 wild type and LCN2$^{-/-}$ mice (6 animals/group) were subjected to a single intraperitoneal injection of CCl_4 (0.8 ml/kg body weight) for 48 h. The serum transaminases AST and ALT were significantly higher in LCN2$^{-/-}$ mice (Fig. 2A). Moreover, inflammatory cytokines and chemokines were expressed at higher levels in LCN2$^{-/-}$ livers (Fig. 2B). Likewise, α-SMA mRNA indicating activation of hepatic stellate cells was higher expressed in livers of respective animals (data not shown). Liver histology showed more inflammatory cell infiltration and fat content in LCN2$^{-/-}$ mice (Fig. 2C). Additionally, TUNEL assay showed more apoptotic hepatocytes around central veins (Fig. 2D).

3.3. LCN2$^{-/-}$ mice are more susceptible to T-cell mediated hepatitis

LCN2 is an acute phase protein in mice and as such part of the innate immune response. Upon induction of immune-mediated acute

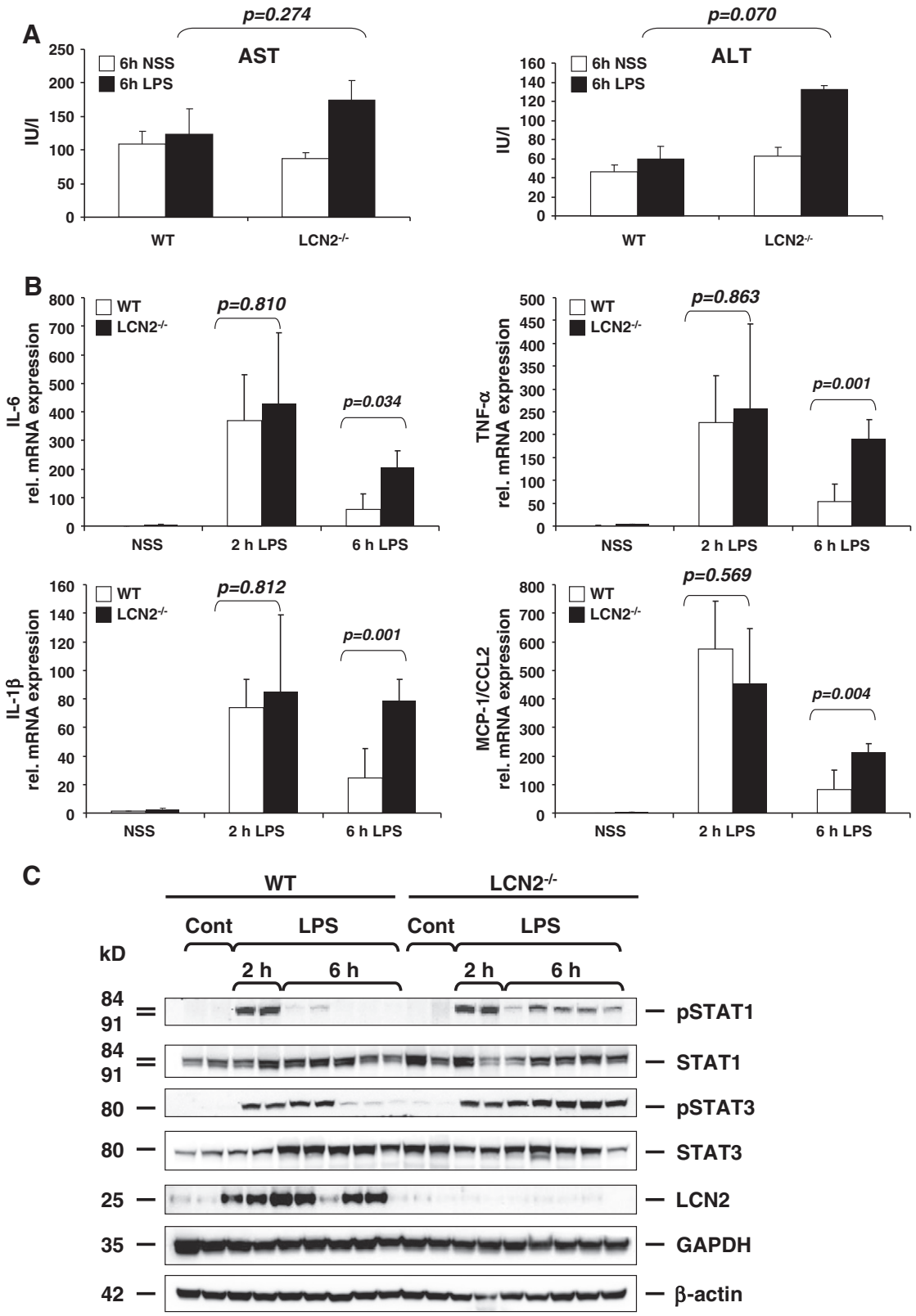

Fig. 4. LCN2$^{-/-}$ mice are prone to more liver damage after LPS injection. (A) Serum AST and ALT were measured in wild type and LCN2 deficient mice at 2 h (*left panel*) and 6 h (*right panel*) after i.p. injection of a single dose LPS (2.5 mg/kg). (B) qRT-PCR showing increased expression of pro-inflammatory cytokines IL-6, TNF-α, IL-1β and MCP-1/CCL2 in LCN2$^{-/-}$ livers compared to controls. (C) Western blot analysis showing sustained phosphorylation of STAT1 and STAT3 in LCN2$^{-/-}$ livers. GAPDH and β-actin served as loading controls.

hepatitis by ConA, LCN2$^{-/-}$ mice exhibited more severe liver damage than their wild-type counterparts that was associated with increased expression levels of pro-inflammatory cytokines including IL-6, TNF-α, IL-1α, IL-1β, IFN-γ, IL-2, and IL-4 while the expression of IL-10 was unaffected (Fig. 3A). In line with the activation of several inflammatory cytokines after ConA challenge, we found strong

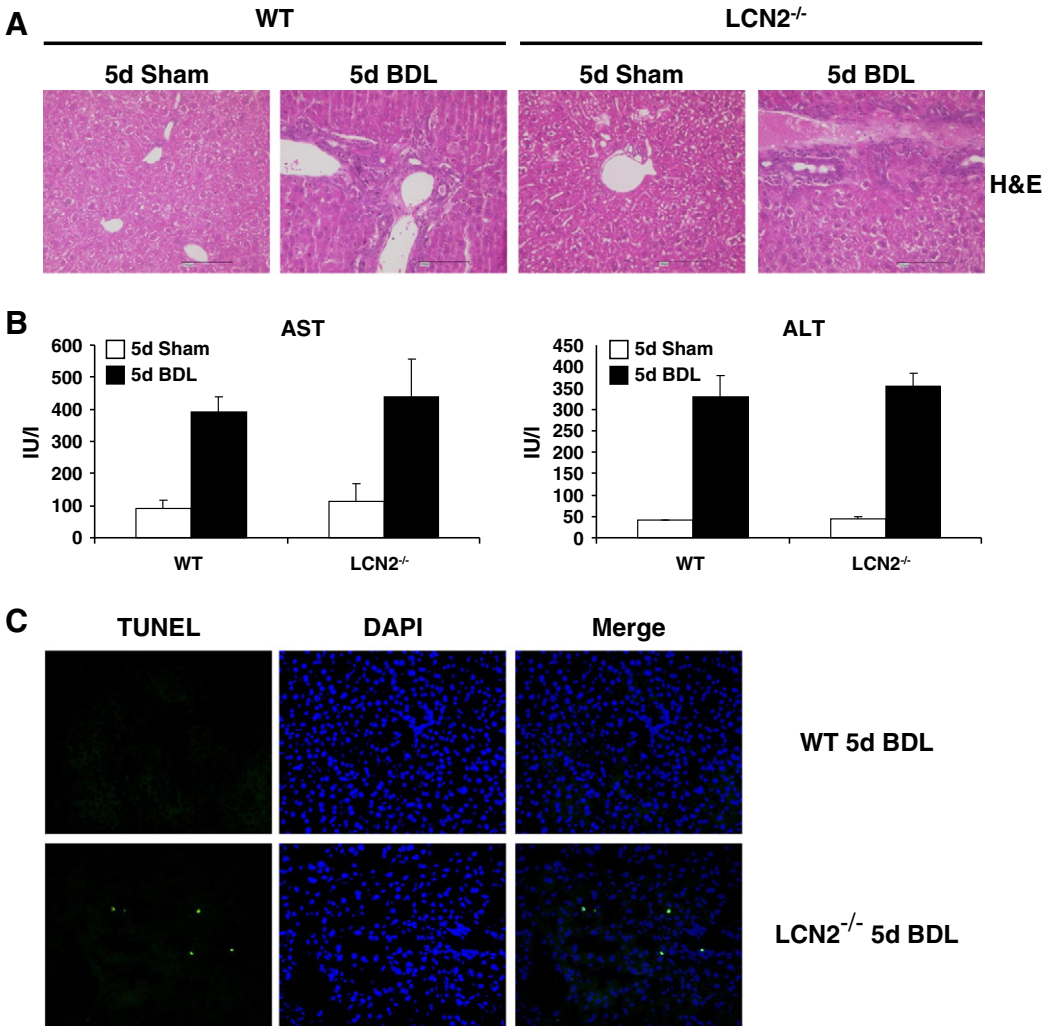

Fig. 5. Increased hepatocyte apoptosis in LCN2$^{-/-}$ mice after 5 day bile duct ligation. (A) H&E staining of liver specimen isolated from mice that were sacrificed 5 days after BDL or sham operation surgery showed more proliferative bile ducts and periportal infiltration of inflammatory cells in LCN2$^{-/-}$ mice than in respective wild type controls. (B) Serum AST and ALT were measured demonstrating no significant differences between wild type and LCN2$^{-/-}$ deficient mice. (C) TUNEL assay showed more hepatocyte apoptosis in LCN2$^{-/-}$ animals compared to control animals. (Magnification 100x).

activation of the STAT1, STAT3, and JNK pathways in respective mice (Fig. 3B).

Interestingly, we noticed that hepatocyte apoptosis was more pronounced in ConA-challenged LCN2$^{-/-}$ mice (Fig. 3C). ConA activates T cells and binds mannose residues of different glycoproteins thereby activating lymphocytes. In this model, immune-mediated liver injury strongly depends on activation of CD4^{+} T cells, NKT cells and Kupffer cells [31]. In line, we found by FACS analysis that hepatic leukocyte isolates significantly more hepatic macrophages and Kupffer cells in mice lacking LCN2 as indicated by increased numbers of cells positive for CD11b and F4/80 (Fig. 3D).

3.4. LCN2$^{-/-}$ mice show enhanced LPS-induced acute liver injury

Bacterial LPS represents a well known agent triggering hepatic injury and subsequent fibrosis. LPS application in mice results in a rapid and marked induction of IL-6, IL-1β and TNF-α promoting hepatocyte damage and HSC activation resulting in inflammation and fibrosis. After application of a single dose of 2.5 mg/kg LPS, serum AST and ALT tended to be increased in LCN2-deficient compared to WT mice (Fig. 4A). In line, the levels of IL-1β, IL-6, TNF-α and MCP-1/CCL2 after 6 h remained higher in LCN2$^{-/-}$ mice (Fig. 4B) resulting in sustained phosphorylation of STAT1 and STAT3 (Fig. 4C).

3.5. More hepatocyte apoptosis in LCN2$^{-/-}$ mice in 5 day-BDL-induced acute liver injury

In early periods of cholestasis induced by BDL, livers showed proliferative bile ducts and periportal infiltration by inflammatory cells (Fig. 5A). In this model, the serum AST and ALT were not significant different between LCN2$^{-/-}$ and control animals (Fig. 5B). However, in line with the observations that we made in the LPS model, TUNEL assays revealed increased hepatocyte apoptosis in LCN2$^{-/-}$ animals (Fig. 5C).

3.6. LCN2$^{-/-}$ mice showed more liver damage after long term CCl_4 application

Mice were injected with CCl_4 twice weekly for 8 weeks. Serum aminotransferases (Fig. 6A), hepatic expression of collagen type I (αI) (Fig. 6B, *left*) and α-SMA mRNA (Fig. 6B, *right*) were higher in LCN2$^{-/-}$ animals (Fig. 6B), but Sirius Red and α-SMA immunohistochemistry staining as well as Western blot analysis showed only

slightly differences in both groups (Fig. 6C–F). However, the levels of several inflammatory cytokines in LCN2$^{-/-}$ mice after treatment with CCl_4 were significantly higher than in WT controls (Fig. 6G). A similar phenomenon was observed when animals were compared after setting BDL for 4 weeks (Fig. 7). Surprisingly, long-term i.p. application of mineral oil did induce sterile peritoneal inflammation and granuloma without liver fibrosis, but also showed significant upregulation of LCN2 in WT mice. Immunohistochemistry of LCN2 confirmed the production of LCN2 in residential (i.e. Kupffer cells) and infiltrating inflammatory cells (i.e. macrophages) in livers of animals that were subjected to application of mineral oil for eight weeks (Suppl. Fig. 1).

3.7. Sustained NFκB activation in LCN2$^{-/-}$ hepatocytes

Since hepatic LCN2 production is induced by IL-1β through NFκB activation [22], we next examined NFκB signaling in LCN2$^{-/-}$ hepatocytes. Therefore, primary cultured hepatocytes were stimulated with IL-1β, IL-6, TNF-α, as well as a combination of IL-1β and IL-6 in Hepatozyme for 30 min and 24 h. Protein cell extracts were prepared and analyzed by Western blot for NFκB signaling components (Fig. 8). Both TNF-α and IL-1β did activate canonical NFκB signaling pathway, evidenced by phosphorylation of IKKα/β, subsequently induced IκBα degradation, and p65 phosphorylation at 30 min. Although we noticed a slight lesser degree of IKKα/β phosphorylation in hepatocytes isolated from LCN2$^{-/-}$ mice, we found no differences in pp65. The 24 h incubation, however, showed sustained p65 phosphorylation in LCN2$^{-/-}$ hepatocytes. Contrary to IL-1β, TNF-α did activate NFκB signaling but failed to induce LCN2 production. Moreover, in LCN2$^{-/-}$ hepatocytes, the stimulation with TNF-α resulted in hepatocyte apoptosis as evidenced by elevated levels of cleaved caspase-3.

3.8. Serum levels of LCN2 in chronic human liver disease

In order to elucidate whether LCN2 is also regulated in human liver disease, we assessed LCN2 serum levels in 192 patients with chronic liver diseases of variable etiology and clinical severity in comparison to 91 healthy controls. LCN2 was readily detectable by ELISA in all samples. Patients with chronic liver disease exhibited significantly higher concentrations compared to the healthy control cohort (median 67.45 ng/mL [range 17.3–401.9] vs. 57.9 ng/mL [range 18.3–176.3]; $p = 0.0127$) (Fig. 9A). Evaluating its usefulness to discriminate between different stages of chronic liver disease, we failed to detect significantly varying levels of LCN2 in non-cirrhotic vs. cirrhotic patients indicating

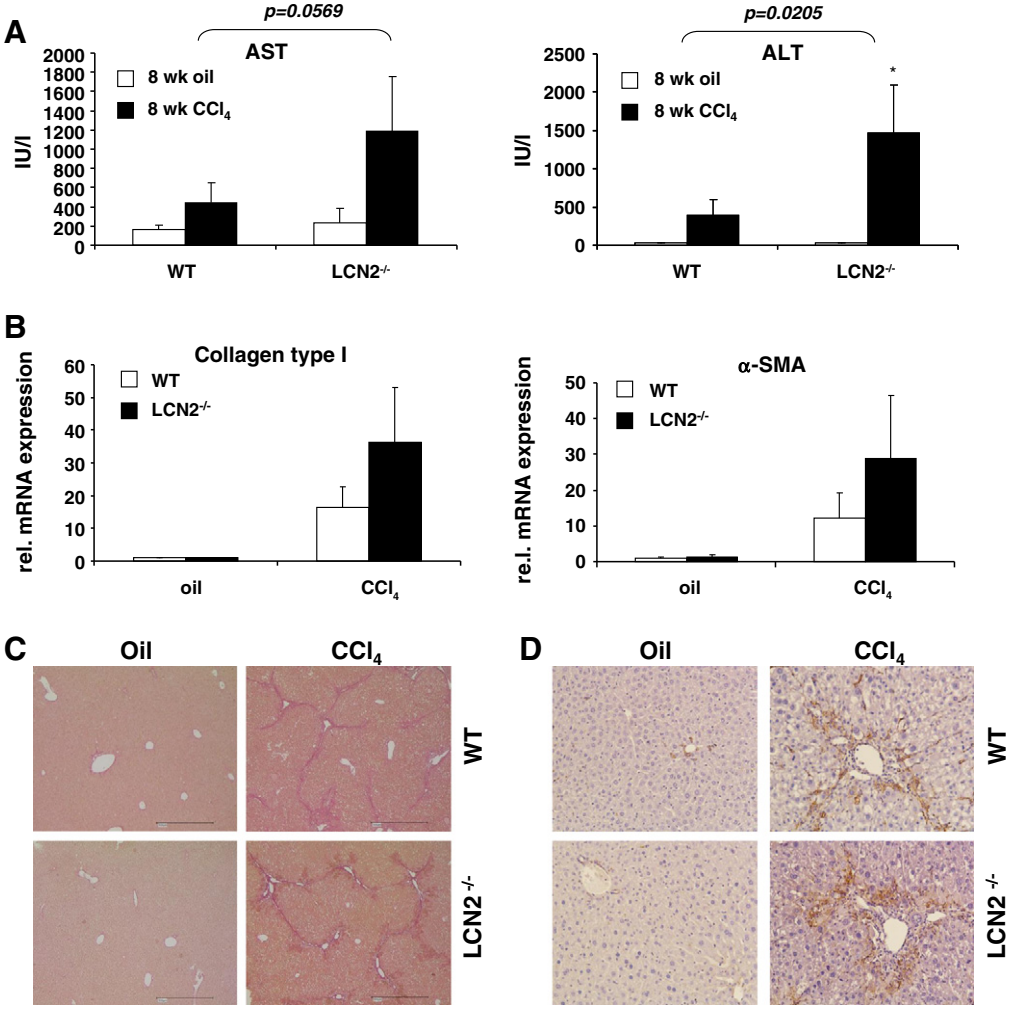

Fig. 6. LCN2$^{-/-}$ mice showed more liver pathology after long term application of CCl_4. (A) Mice were treated for 8 weeks with CCl_4 twice weekly while mineral oil served as control and serum AST (*left panel*) and ALT (*right panel*) measured. (B) qRT-PCR showing increased collagen type I (*left panel*) and α-SMA (*right panel*) mRNA expression in CCl_4-treated LCN2$^{-/-}$ mice compared to wild type controls. (C, D) Liver specimen were stained with (C) Sirius Red or analyzed for (D) α-SMA expression in immunohistochemistry. (E) Liver protein lysates were analyzed for expression of fibrotic marker proteins (i.e. fibronectin, collagen type I, and α-SMA) in Western blot. rS6 and β-actin served as loading controls. Each lane represents one individual mouse. Please note that LCN2 expression in liver was upregulated after injection of both mineral oil and CCl_4. (F) The amounts of collagen type I (*left*) and α-SMA (*right*) obtained in Western blot analysis (E) were quantified densitometrically. (G) qRT-PCR of pro-inflammatory cytokines after 8 week treatment with CCl_4 revealed that CCL2, CCR2, IL-1β, and TNF-α show increased levels in livers of LCN2$^{-/-}$ mice.

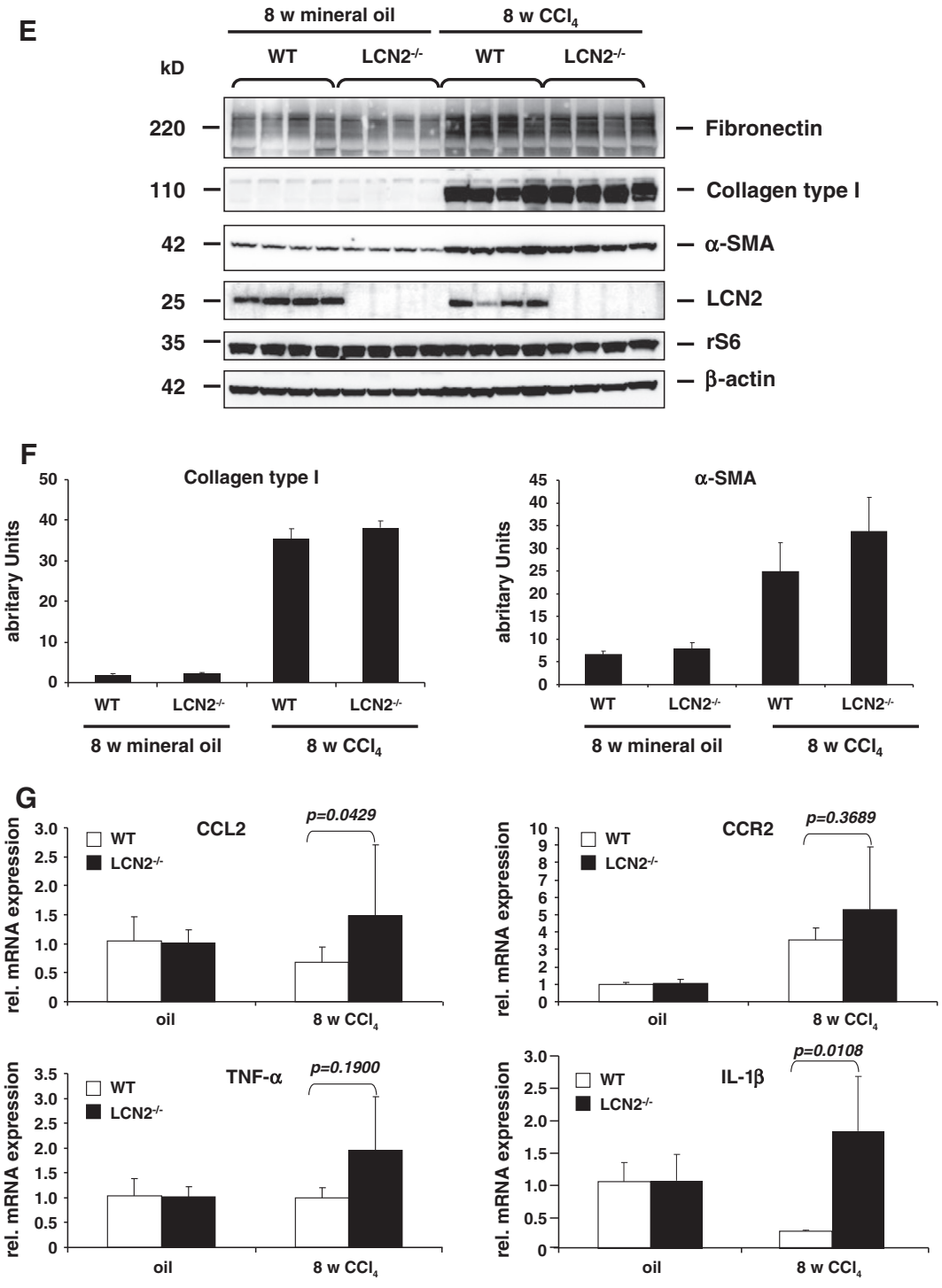

Fig. 6 (*continued*).

that serum LCN2 does not reflect stage of chronic liver disease (Fig. 9B). Accordingly, patients with underlying compensated cirrhosis (Child A) displayed comparable levels of circulating LCN2 to those with end-stage liver disease (Child C) (Fig. 9C). In line, correlation analysis did not reveal associations between LCN2 and serum markers of liver synthesis capacity (albumin, PCHE, INR, and Factor V), cholestasis (bilirubin), liver-related enzymes as indicators of hepatocellular cell damage (AST, ALT, and GLDH) and non-invasive fibrosis markers (hyaluronic acid and procollagen-III-peptide) as well as composite scores for assessment of end-stage liver disease (Child–Pugh-Score points, MELD score) (Table 3). Etiology of underlying disease neither had a detectable influence on serum LCN2 concentrations even when adjusted to liver function (Fig. 9D and data not shown). However, there is substantial evidence that LCN2 elevation occurs in the context of inflammation which is frequently present in chronic liver disease since various acute-phase proteins (CRP and ferritin), white blood cell count, cytokines (TNF-α and IL-6) and inflammatory cytokines (MIP-1α, MIP-1β, MCP-1, and IL-8) positively correlated with serum LCN2 concentrations. Serum LCN2 levels showed no correlation with serum ALT (Fig. 9E) and AST (Fig. 9F) but was additionally

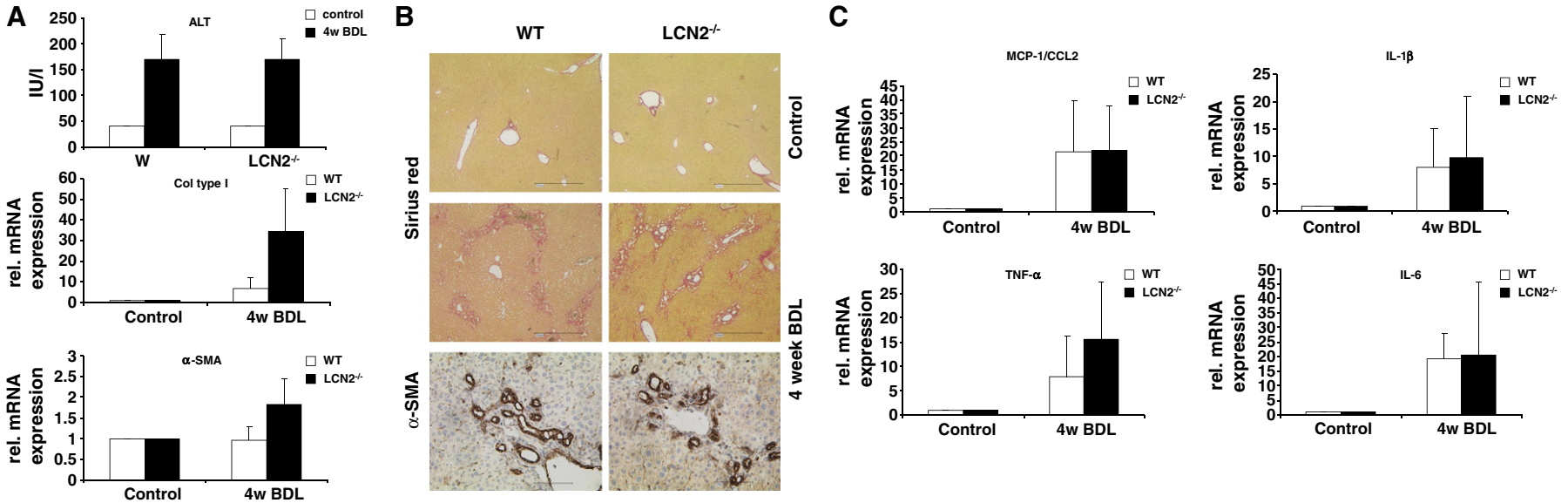

Fig. 7. Induction of slightly more fibrosis in LCN2$^{-/-}$ mice. (A) Serum ALT (*upper panel*) was measured in wild type and LCN2$^{-/-}$ mice that were kept for 4 weeks after sham and BDL operation reflecting no significant differences between both groups. However, quantitative real time PCR showed increased collagen type I (*middle panel*) and α-SMA (*lower panel*) mRNA expression in BDL-treated LCN2$^{-/-}$ mice compared to controls. (B) Sirius red and α-SMA immunohistochemistry staining of sham-operated and 4 w BDL livers reflecting slightly increased fibrosis in LCN2$^{-/-}$ mice. Bars represent 500 μM. (C) Quantitative real time showed no differences in mRNA expression of pro-inflammatory cytokines (i.e. MCP-1/CCL2, IL-1β, TNF-α, and IL-6) between the LCN2$^{-/-}$ and wild type control group.

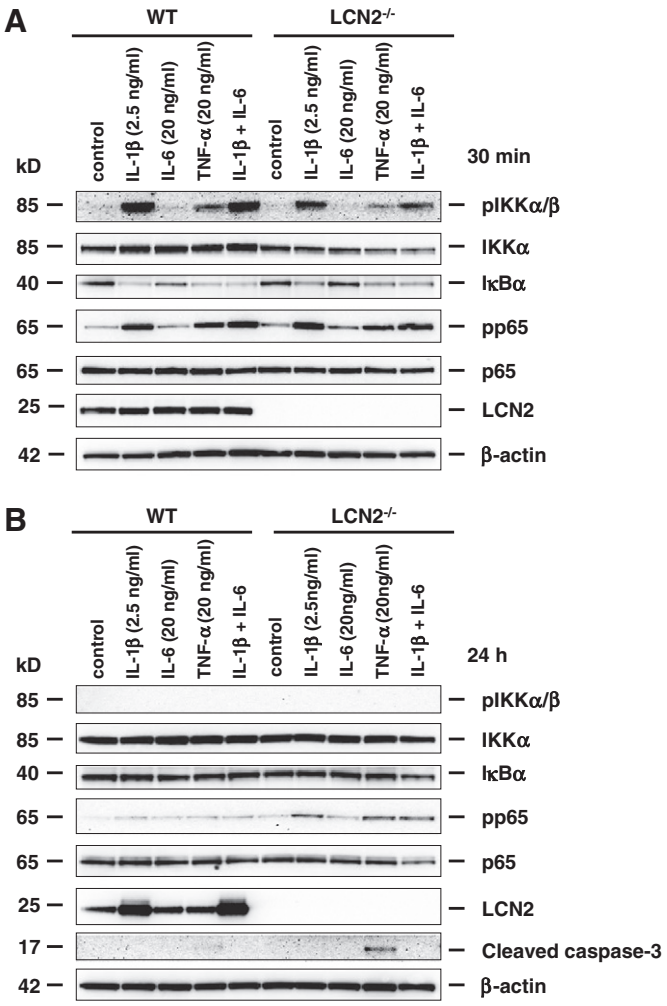

Fig. 8. Sustained NFκB activation in LCN2$^{-/-}$ hepatocytes. Primary hepatocytes from wild type and LCN2-deficient mice were stimulated with IL-1β, IL-6, TNF-α, and IL-1β/IL-6 for 30 min (A) and 24 h (B) or left unstimulated (*control*). Protein extracts were prepared and analyzed for signaling components of the canonical NFκB signaling pathway by Western blot.

related to impaired renal function in patients with chronic liver disease given the close correlations to urea and glomerular filtration rate (GFR) as calculated by cystatin C measurements and the significant LCN2 increase in patients with a GFR below 60 ml/min/1.73 m^2 (Table 3 and Fig. 9G). Selecting patients with a creatinine value below 1.5 mg/dL LCN2 turned out to be a useful marker to detect patients with a cystatin-C-based GFR under 50 ml/min/1.73 m^2 in a ROC-curve analysis (AUC 0.652, p = 0.015).

4. Discussion

LCN2 is an acute phase protein in mice. We here examined LCN2 expression in different acute liver injury models within the first 24 h and found that LCN2 increases after application of CCl_4, ConA and LPS. Interestingly, the levels of hepatic and serum LCN2 correlated well with serum AST and ALT confirming a previous finding that human serum LCN2 correlates significantly with AST, ALT, cholesterol, creatinine and C-reactive protein [32]. Additionally, the LCN2 levels in our analysis also corresponded to CCL2 mRNA representing a marker of inflammation.

Serum and urinary LCN2 are now accepted as a sensitivity marker in early stage of acute kidney injury that is independent of serum creatinine [33,16]. The specific function of LCN2 in kidney injury, as a nephroprotective- or a profibrogenic factor is still under debate [14,15].

In liver, the precise function of LCN2 is still enigmatic. We here used LCN2$^{-/-}$ mice to explore the functional roles of LCN2 in different experimental liver injury models. Targeted disruption of the murine *LCN2* gene is compatible with normal organogenesis and development to adulthood [20]. In line, we found no differences in liver function tests in healthy animals compared to wild type controls. However, during the challenge with acute toxic chemicals or the generation of mechanical induced cholestasis, LCN2$^{-/-}$ mice showed significantly more liver damage as evidenced by increased AST and ALT after application of CCl_4, ConA and LPS, while the BDL surgery in short-term revealed no differences in both groups. This suggests that rapid LCN2 induction protects hepatocytes from direct toxic injury. In contrast, hepatocyte injury resulting from the BDL surgery is more gradual during the progression of cholestasis and LCN2 is produced mainly from proliferative bile duct epithelia.

Additionally, the chemically-induced injury exhibited more inflammatory responses compared to the mechanically induced BDL as evidenced by more infiltrating inflammatory cells as evidenced by immunohistochemistry (Suppl. Fig. 1) and upregulation of the pro-inflammatory cytokines IL-1β, IL-6, TNF-α and IFN-γ. The LCN2$^{-/-}$ mice expressed higher levels of the respective cytokines, including the MCP-1/CCL2 chemokine, while the anti-inflammatory cytokine IL-10 actually decreased or remained unchanged.

In the ConA and LPS models, IFN-γ is the major cytokine responsible for STAT1 activation. STAT1 not only plays a key role in antiviral defense during hepatitis virus infection but also contributes to liver inflammation and injury and suppression of liver regeneration. We

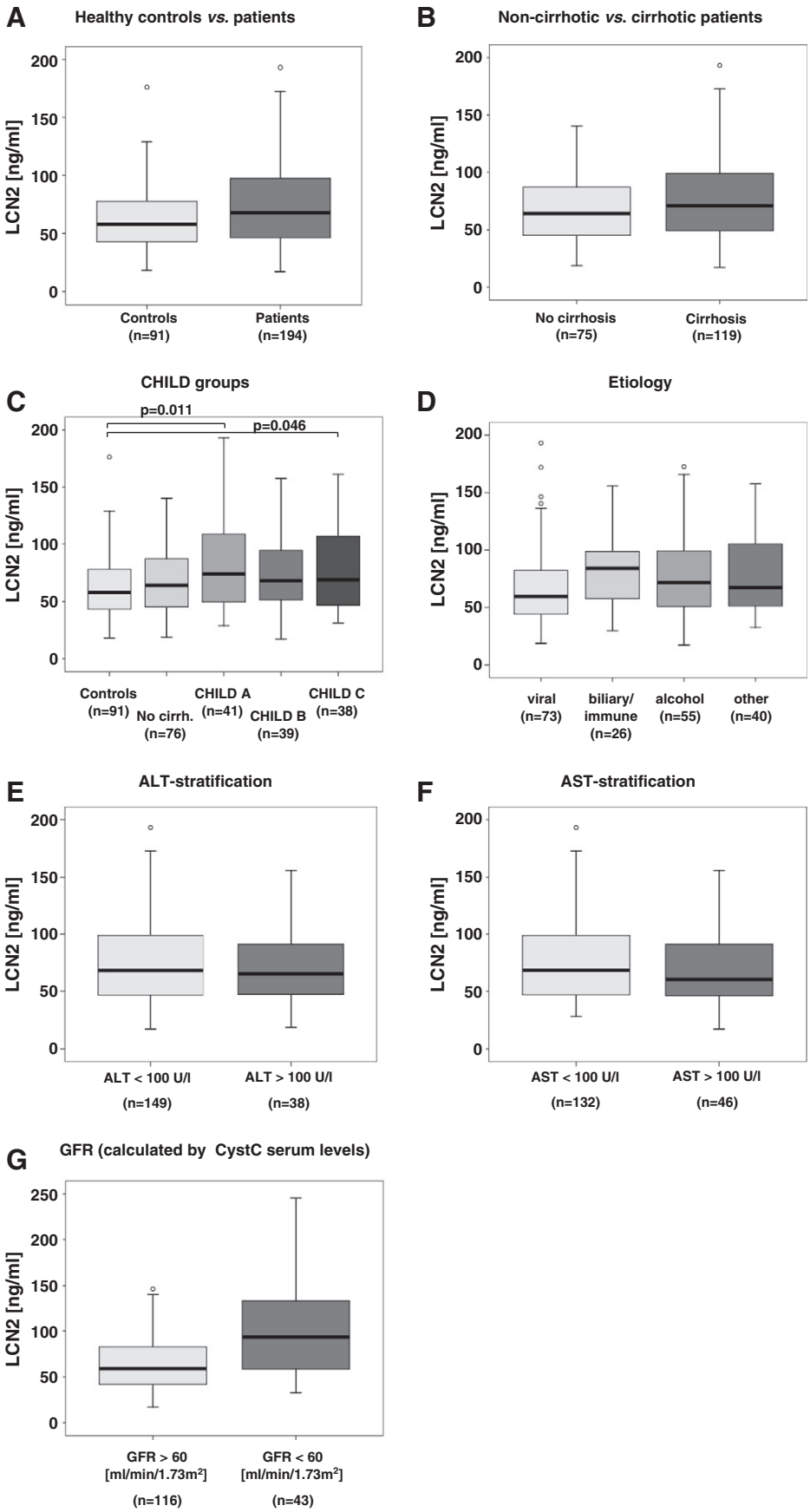

Fig. 9. Serum LCN2 in liver disease patients. (A) Serum LCN2 values in patients suffering from various liver diseases were significantly higher than in control patients ($p = 0.010$). (B) No significant differences in LCN2 serum levels were observed between cirrhotic and non-cirrhotic patients. (C) The group of patients with Child A and Child C however showed significant higher levels of LCN2 compared to healthy control-patients. (D) Serum LCN2 levels were not different between the initiating causes of the diseases, and showed no correlation with serum AST (E) and ALT (F). (G) By contrast, LCN2 showed a significant inverse correlation with the glomerular filtration rate (GFR).

Table 3
LCN2 correlation analysis [patients only].

Parameter	Correlation coefficient *r*	p-value
MIP-1α	.232	.006
MIG	.212	.016
MCP-1	.221	.012
IP-10	.199	.030
IL-8	.225	.002
IL-6	.267	.001
Urea	.388	<.001
Cystatin C	.274	<.001
GFR [Cystatin C]	−.274	<.001
Uric acid	.207	.007
CRP	.244	.001
PCT	.266	.001
WBC	.430	<.001
Lymphocytes [rel. count]	−.390	<.001
IL-10	.212	.007
TNF-α	.187	.019
Monocytes [rel. PBMC]	.221	.003

found STAT1 phosphorylation in both LCN2$^{-/-}$ and wild type mice, but STAT1 showed sustained activation in LCN2$^{-/-}$ mice after LPS challenge, possibly being causative for more severe liver damage that we noticed in our analysis.

STAT3 is activated by a wide variety of cytokines (e.g. IL-6) and viral proteins and plays a key role in acute phase response, promotion of regeneration, glucose homeostasis, and hepatic lipid metabolism and protects against liver injury by suppression of IFN-γ signaling [34,35]. Since IL-6 is also one of the cytokines inducing LCN2 expression in cultured hepatocytes [22], LCN2 might be involved in the mediation of hepatoprotective effects downstream of IL-6 and STAT3.

TNF-α and IL-1β are mainly released from activated Kupffer cells or infiltrating neutrophils and macrophages. Both elicit defensive responses in parenchymal cells, including activation of apoptosis but when these defensive responses are overwhelming, cells may die by necrosis and thereby stimulate even more inflammatory responses. Following toxic chemical injury, LCN2$^{-/-}$ mice expressed higher levels of these cytokines, culminating in more severe liver damage. TNF-α induces specific signaling pathways in hepatocytes that lead to activation of either pro-survival mediators or effectors of cell death. Whereas activation of transcription factor NFκB promotes cell survival, c-Jun N-terminal kinases (JNK) and caspases are strategic effectors of cell death in the TNF-α-mediated signaling pathway.

Notably, stimulation with TNF-α and IL-1β induced prolonged NFκB activation in LCN2$^{-/-}$ hepatocytes (Fig. 8B). This phenomenon might be due to the lack of NFκB negative feedback loops from LCN2 since our previous work showed that NFκB is necessary for LCN2 production [22]. Additionally, the persistence of NFκB activation may explain the higher degree of inflammation that we observed in LCN2$^{-/-}$ mice upon liver injuries.

In order to confirm whether LCN2 levels are also modulated in patients with human liver disease, we assessed LCN2 serum concentrations in a large, well-characterized patient cohort. To our knowledge, this is the first systematic analysis of circulating LCN2 in chronic liver disease patients. Though there was an increase of LCN2 levels in patients compared to the non-diseased, LCN2 levels did not vary within the different stages of liver disease, ranging from non-fibrosis to decompensated liver cirrhosis. These findings might reflect the results of a recent in vitro study from our group indicating that the pro-inflammatory cytokine IL-1β but not the pro-fibrotic mediators PDGF and TGF-β induce LCN2 production in hepatocytes [22].

In support, LCN2 levels correlated with polymorphonuclear cell count, a multitude of parameters indicating acute phase responses and immune cell activation, which corroborates with findings from previous works, that could demonstrate a close link of LCN2 serum levels to sterile and non-sterile inflammatory disease patterns [36–38]. This phenomenon was further observed in our long-term i.p. mineral oil-induced sterile peritoneal inflammation in WT mice showing high levels of LCN2 expression in Western blot and immunohistochemistry. Recent studies showed LCN2 as an important paracrine chemoattractant that stimulates polymorphonuclear cell migration and adherence [39] and actively preventing sepsis [40]. New data further indicate that different leukocyte subset compositions result in alterations of circulating LCN2 levels that may explain why we in contrast to other reports did not find the correlation of serum LCN2 to the staging of chronic liver disease progression [41]. Noteworthy, sustained inflammation, even on a subclinical level, is a hallmark feature of liver fibrosis and cirrhosis. Furthermore, LCN2 concentrations denoted renal insufficiency in our study cohort in congruence to growing evidence that LCN2 is valuable marker of impaired kidney function in liver-related disease settings such as liver transplantation and cirrhosis [42,43]. According to our data and findings by Gerbes et al., LCN2 may detect clinically relevant renal insufficiency in clinical liver disease patients when serum creatinine levels would only indicate a modest functional decline. Impairment of kidney function is common in cirrhosis and current studies show that patients with hepatic cirrhosis and acute tubular necrosis show strongly increased urine LCN2 levels compared to patients with cirrhosis and classical type 1 hepatorenal syndrome (HRS), but this does not apply to HRS patients with active bacterial infections. Moreover, patients with classical type 1 HRS show higher urine LCN2 levels compared to type 2 HRS patients, chronic kidney diseases, and pre-renal azotemia, due to volume depletion. Urine LCN2 levels therefore may be indicative in the differential diagnosis of kidney function impairment in liver cirrhosis [44,45]. Even though systemic LCN2 levels were not directly associated to liver function and disease severity, it is conceivable that LCN2 is regulated locally in response to acute or chronic damage in human livers. More studies comprising evaluation of hepatic LCN2 expression in liver biopsies or explants are therefore essential to further elucidate the precise role and regulation of LCN2 in human liver disease. The study presented here, however, already demonstrates that LCN2 is functionally linked to the process of inflammatory liver disease and it is reasonable to speculate that this lipocalin is an important mediator that in conjunction with other molecular mediators and pathways regulates and controls liver homeostasis (Suppl. Fig. 2).

In conclusion, upregulation of LCN2 in liver has several aspects: (i) it is a reliable indicator of liver damage, (ii) it has a significant hepatoprotective effect in acute liver injury, and (iii) LCN2 levels provide no correlation to the degree of liver fibrosis but provide a significant positive correlation to inflammation.

Supplementary data to this article can be found online at http://dx.doi.org/10.1016/j.bbadis.2013.01.014.

References

[1] D.R. Flower, The lipocalin protein family: structure and function, Biochem. J. 318 (1996) 1–14.
[2] S. Hraba-Renevey, H. Türler, M. Kress, C. Salomon, R. Weil, SV40-induced expression of mouse gene 24p3 involves a post-transcriptional mechanism, Oncogene 4 (1989) 601–608.
[3] L. Kjeldsen, A.H. Johnsen, H. Sengeløv, N. Borregaard, Isolation and primary structure of NGAL, a novel protein associated with human neutrophil gelatinase, J. Biol. Chem. 268 (1993) 10425–10432.
[4] T. Bratt, Lipocalins and cancer, Biochim. Biophys. Acta 1482 (2000) 318–326.
[5] T. Berger, C.C. Cheung, A.J. Elia, T.W. Mak, Disruption of the Lcn2 gene in mice suppresses primary mammary tumor formation but does not decrease lung metastasis, Proc. Natl. Acad. Sci. U. S. A. 107 (2010) 2995–3000.
[6] X. Leng, T. Ding, H. Lin, Y. Wang, L. Hu, J. Hu, B. Feig, W. Zhang, L. Pusztai, W.F. Symmans, Y. Wu, R.B. Arlinghaus, Inhibition of lipocalin 2 impairs breast tumorigenesis and metastasis, Cancer Res. 69 (2009) 8579–8584.
[7] V.R. Sunil, K.J. Patel, M. Nilsen-Hamilton, D.E. Heck, J.D. Laskin, D.L. Laskin, Acute endotoxemia is associated with upregulation of lipocalin 24p3/Lcn2 in lung and liver, Exp. Mol. Pathol. 83 (2007) 177–187.
[8] J. Yang, K. Mori, J.Y. Li, J. Barasch, Iron, lipocalin, and kidney epithelia, Am. J. Physiol. Renal Physiol. 285 (2003) F9–F18.
[9] L. Kjeldsen, J.B. Cowland, N. Borregaard, Human neutrophil gelatinase-associated lipocalin and homologous proteins in rat and mouse, Biochim. Biophys. Acta 1482 (2000) 272–283.
[10] Z. Tong, X. Wu, J.P. Kehrer, Increased expression of the lipocalin 24p3 as an apoptotic mechanism for MK886, Biochem. J. 372 (2003) 203–210.

[11] Z. Tong, X. Wu, D. Ovcharenko, J. Zhu, C.S. Chen, J.P. Kehrer, Neutrophil gelatinase-associated lipocalin as a survival factor, Biochem. J. 391 (2005) 441–448.
[12] K.M. Schmidt-Ott, K. Mori, A. Kalandadze, J.Y. Li, N. Paragas, T. Nicholas, P. Devarajan, J. Barasch, Neutrophil gelatinase-associated lipocalin-mediated iron traffic in kidney epithelia, Curr. Opin. Nephrol. Hypertens. 15 (2006) 442–449.
[13] J. Mishra, K. Mori, Q. Ma, C. Kelly, J. Yang, M. Mitsnefes, J. Barasch, P. Devarajan, Amelioration of ischemic acute renal injury by neutrophil gelatinase-associated lipocalin, J. Am. Soc. Nephrol. 15 (2004) 3073–3082.
[14] K. Mori, H.T. Lee, D. Rapoport, I.R. Drexler, K. Foster, J. Yang, K.M. Schmidt-Ott, X. Chen, J.Y. Li, S. Weiss, J. Mishra, F.H. Cheema, G. Markowitz, T. Suganami, K. Sawai, M. Mukoyama, C. Kunis, V. D'Agati, P. Devarajan, J. Barasch, Endocytic delivery of lipocalinsiderophore–iron complex rescues the kidney from ischemia–reperfusion injury, J. Clin. Invest. 115 (2005) 610–621.
[15] G. Bao, M. Clifton, T.M. Hoette, K. Mori, S.X. Deng, A. Qiu, M. Viltard, D. Williams, N. Paragas, T. Leete, R. Kulkarni, X. Li, B. Lee, A. Kalandadze, A.J. Ratner, J.C. Pizarro, K.M. Schmidt-Ott, D.W. Landry, K.N. Raymond, R.K. Strong, J. Barasch, Iron traffics in circulation bound to a siderocalin (Ngal)–catechol complex, Nat. Chem. Biol. 6 (2010) 602–609.
[16] K.M. Schmidt-Ott, Neutrophil gelatinase-associated lipocalin as a biomarker of acute kidney injury—where do we stand today? Nephrol. Dial. Transplant. 26 (2011) 762–764.
[17] A. Viau, K. El Karoui, D. Laouari, M. Burtin, C. Nguyen, K. Mori, E. Pillebout, T. Berger, T.W. Mak, B. Knebelmann, G. Friedlander, J. Barasch, F. Terzi, Lipocalin 2 is essential for chronic kidney disease progression in mice and humans, J. Clin. Invest. 120 (2010) 4065–4076.
[18] D.H. Goetz, M.A. Holmes, N. Borregaard, M.E. Bluhm, K.N. Raymond, R.K. Strong, The neutrophil lipocalin NGAL is a bacteriostatic agent that interferes with siderophore-mediated iron acquisition, Mol. Cell 10 (2002) 1033–1043.
[19] T.H. Flo, K.D. Smith, S. Sato, D.J. Rodriguez, M.A. Holmes, R.K. Strong, S. Akira, A. Aderem, Lipocalin 2 mediates an innate immune response to bacterial infection by sequestrating iron, Nature 432 (2004) 917–921.
[20] T. Berger, A. Togawa, G.S. Duncan, A.J. Elia, A. You-Ten, A. Wakeham, H.E. Fong, C.C. Cheung, T.W. Mak, Lipocalin 2-deficient mice exhibit increased sensitivity to *Escherichia coli* infection but not to ischemia–reperfusion injury, Proc. Natl. Acad. Sci. U. S. A. 103 (2006) 1834–1839.
[21] C. Ratledge, Iron metabolism and infection, Food Nutr. Bull. 28 (2007) S515–S523.
[22] E. Borkham-Kamphorst, F. Drews, R. Weiskirchen, Induction of lipocalin-2 expression in acute and chronic experimental liver injury moderated by pro-inflammatory cytokines interleukin-1β through nuclear factor-κB activation, Liver Int. 31 (2011) 656–665.
[23] M.H. Roudkenar, Y. Kuwahara, T. Baba, A.M. Roushandeh, S. Ebishima, S. Abe, Y. Ohkubo, M. Fukumoto, Oxidative stress induced lipocalin 2 gene expression: addressing its expression under the harmful conditions, J. Radiat. Res. 48 (2007) 39–44.
[24] E. Borkham-Kamphorst, S. Huss, E. Van de Leur, U. Haas, R. Weiskirchen, Adenoviral CCN3/NOV gene transfer fails to mitigate liver fibrosis in an experimental bile duct ligation model because of hepatocyte apoptosis, Liver Int. 32 (2012) 1342–1353.
[25] H.W. Zimmermann, S. Seidler, J. Nattermann, N. Gassler, C. Hellerbrand, A. Zernecke, J.J. Tischendorf, T. Luedde, R. Weiskichen, C. Trautwein, F. Tacke, Functional contribution of elevated circulating and hepatic non-classical CD14CD16 monocytes to inflammation and human liver fibrosis, PLoS One 5 (6) (2010) e11049.
[26] F. Tacke, G. Brabant, E. Kruck, R. Horn, P. Schöffski, H. Hecker, M.P. Manns, C. Trautwein, Ghrelin in chronic liver disease, J. Hepatol. 38 (2003) 447–454.
[27] K.R. Karlmark, R. Weiskirchen, H.W. Zimmermann, N. Gassler, F. Ginhoux, C. Weber, M. Merad, T. Luedde, C. Trautwein, F. Tacke, Hepatic recruitment of the inflammatory $Gr1^{+}$ monocyte subset upon liver injury promotes hepatic fibrosis, Hepatology 50 (2009) 261–274.
[28] J. Kountouras, B.H. Billing, P.J. Scheuer, Prolonged bile duct obstruction: a new experimental model for cirrhosis in the rat, Br. J. Exp. Pathol. 65 (1984) 305–311.
[29] M. Arias, S. Sauer-Lehnen, J. Treptau, N. Janoschek, I. Theuerkauf, R. Buettner, A.M. Gressner, R. Weiskirchen, Adenoviral expression of a transforming growth factor-beta1 antisense mRNA is effective in preventing liver fibrosis in bile-duct ligated rats, BMC Gastroenterol. 3 (2003) 29.
[30] E. Borkham-Kamphorst, E. Kovalenko, C.R. van Roeyen, N. Gassler, M. Bomble, T. Ostendorf, J. Floege, A.M. Gressner, R. Weiskirchen, Platelet-derived growth factor isoform expression in carbon tetrachloride-induced chronic liver injury, Lab. Invest. 88 (2008) 1090–1100.
[31] K. Takeda, Y. Hayakawa, L. Van Kaer, H. Matsuda, H. Yagita, K. Okumura, Critical contribution of liver natural killer T cells to a murine model of hepatitis, Proc. Natl. Acad. Sci. U. S. A. 97 (2000) 5498–5503.
[32] D. Stejskal, M. Karpísek, V. Humenanska, Z. Hanulova, P. Stejskal, P. Kusnierova, M. Petzel, Lipocalin-2: development, analytical characterization, and clinical testing of a new ELISA, Horm. Metab. Res. 40 (2008) 381–385.
[33] M. Haase, P.R. Mertens, Urinary biomarkers—silver bullets to faster drug development and nephron protection, Nephrol. Dial. Transplant. 25 (2010) 3167–3169.
[34] H. Wang, F. Lafdil, X. Kong, B. Gao, Signal transducer and activator of transcription 3 in liver diseases: a novel therapeutic target, Int. J. Biol. Sci. 7 (2011) 536–550.
[35] F. Hong, B. Jaruga, W.H. Kim, S. Radaeva, O.N. El-Assal, Z. Tian, V.A. Nguyen, B. Gao, Opposing roles of STAT1 and STAT3 in T cell-mediated hepatitis: regulation by SOCS, J. Clin. Invest. 110 (2002) 1503–1513.
[36] S. Sultan, M. Pascucci, S. Ahmad, I.A. Malik, A. Bianchi, P. Ramadori, G. Ahmad, G. Ramadori, LIPOCALIN-2 is a major acute-phase protein in a rat and mouse model of sterile abscess, Shock 37 (2012) 191–196.
[37] S. Chakraborty, S. Kaur, V. Muddana, N. Sharma, U.A. Wittel, G.I. Papachristou, D. Whitcomb, R.E. Brand, S.K. Batra, Elevated serum neutrophil gelatinase-associated lipocalin is an early predictor of severity and outcome in acute pancreatitis, Am. J. Gastroenterol. 105 (2010) 2050–2059.
[38] N.I. Shapiro, S. Trzeciak, J.E. Hollander, R. Birkhahn, R. Otero, T.M. Osborn, E. Moretti, H.B. Nguyen, K.J. Gunnerson, D. Milzman, D.F. Gaieski, M. Goyal, C.B. Cairns, L. Ngo, E.P. Rivers, A prospective, multicenter derivation of a biomarker panel to assess risk of organ dysfunction, shock, and death in emergency department patients with suspected sepsis, Crit. Care Med. 37 (2009) 96–104.
[39] A. Schroll, K. Eller, C. Feistritzer, M. Nairz, T. Sonnweber, P.A. Moser, A.R. Rosenkranz, I. Theurl, G. Weiss, Lipocalin-2 ameliorates granulocyte functionality, Eur. J. Immunol. 42 (2012) 3346–3357.
[40] G. Srinivasan, J.D. Aitken, B. Zhang, F.A. Carvalho, B. Chassaing, R. Shashidharamurthy, N. Borregaard, D.P. Jones, A.T. Gewirtz, M. Vijay-Kumar, Lipocalin 2 deficiency dysregulates iron homeostasis and exacerbates endotoxin-induced sepsis, J. Immunol. 189 (2012) 1911–1919.
[41] G. Lippi, G.L. Salvagno, G. Banfi, Serum but not urine concentration of neutrophil gelatinase-associated lipocalin is influenced by acute leukocyte variations, Leuk. Lymphoma 53 (2012) 1643–1645.
[42] C.U. Niemann, A. Walia, J. Waldman, M. Davio, J.P. Roberts, R. Hirose, J. Feiner, Acute kidney injury during liver transplantation as determined by neutrophil gelatinase-associated lipocalin, Liver Transpl. 15 (2009) 1852–1860.
[43] A.L. Gerbes, A. Benesic, M. Vogeser, A. Krag, F. Bendtsen, S. Møller, Serum neutrophil gelatinase-associated lipocalin — a sensitive novel marker of renal impairment in liver cirrhosis? Digestion 84 (2011) 82–83.
[44] C. Fagundes, M.N. Pépin, M. Guevara, R. Barreto, G. Casals, E. Solà, G. Pereira, E. Rodríguez, E. Garcia, V. Prado, E. Poch, W. Jiménez, J. Fernández, V. Arroyo, P. Ginès, Urinary neutrophil gelatinase-associated lipocalin as biomarker in the differential diagnosis of impairment of kidney function in cirrhosis, J. Hepatol. 57 (2012) 267–273.
[45] E.C. Verna, R.S. Brown, E. Farrand, E.M. Pichardo, C.S. Forster, D.A. Sola-Del Valle, S.H. Adkins, M.E. Sise, J.A. Oliver, J. Radhakrishnan, J.M. Barasch, T.L. Nickolas, Urinary neutrophil gelatinase-associated lipocalin predicts mortality and identifies acute kidney injury in cirrhosis, Dig. Dis. Sci. 57 (2012) 2362–2370.